RECENT RESULTS FROM PROTON INTERMITTENCY ANALYSIS IN NUCLEUS–NUCLEUS COLLISIONS FROM NA61 AT CERN SPS*

N. Davis

for the NA61/SHINE Collaboration

Institute of Nuclear Physics Polish Academy of Sciences, 31-342 Kraków, Poland

N. Antoniou, F.K. Diakonos

Faculty of Physics, University of Athens
University Campus, Zografou, 15-784 Athens, Greece

The search for experimental signatures of the critical point (CP) of strongly interacting matter is one of the main objectives of the NA61/SHINE experiment at CERN SPS. In the course of the experiment, an energy (beam momentum $13A$–$150A$ GeV/c) and system size (p+p, p+Pb, Be+Be, Ar+Sc, Xe+La) scan is performed. Local proton density fluctuations in transverse momentum space represent an order parameter of the chiral phase transition and are expected to scale according to a universal power-law in the vicinity of the CP; we probe their behaviour through an intermittency analysis of the proton second scaled factorial moments (SSFMs) in transverse momentum space. Previous such analyses revealed power-law behaviour in NA49 "Si"+Si collisions at $158A$ GeV/c; no intermittency was observed in NA49 "C"+C and Pb+Pb collisions at the same energy, and in NA61/SHINE Be+Be collisions at $150A$ GeV/c. Results suggest a baryochemical potential for the critical point in the vicinity of ~ 250 MeV. In the present work, we extend the analysis to the NA61/SHINE Ar+Sc system at $150A$ GeV/c. We employ statistical techniques to subtract non-critical background and estimate statistical and systematic uncertainties. Finally, we use Monte Carlo simulations to estimate the likelihood of a spurious signal.

---

1. Introduction

Experimental observables suitable for detecting the CP of strongly interacting matter [1] can be divided into two large categories: on the one hand, event-by-event (global) fluctuations of integrated quantities [2–4]; on the other hand, local power-law fluctuations [5] of the order parameter of the QCD chiral phase transition, the chiral condensate $\langle \bar{q}q \rangle$. The sigma field $\sigma(\boldsymbol{x})$ carries the critical properties of the chiral condensate, and may be reconstructed and probed through its decay into experimentally observable (π^+, π^-) pairs [6]. At finite baryochemical potential, critical fluctuations are also transferred to the net proton density, as well as to the proton and antiproton densities separately [7].

At the CP, the fluctuations of the order parameter are self-similar [8], their singular part governed by the 3D-Ising universality class, and can be detected through an intermittency analysis of proton density fluctuations in transverse momentum space by the use of scaled factorial moments (SFMs). A detailed analysis, supplemented by specially adapted statistical techniques, can be found in Ref. [9], where several heavy-nuclei collision datasets are studied that were recorded in the NA49 experiment at maximum energy ($158A$ GeV/c, $\sqrt{s_{NN}} \approx 17$ GeV) of the SPS (CERN).

2. Method of analysis

Intermittency is defined as the power-law scaling of the second scaled factorial moments (SSFMs) of protons as a function of bin size in transverse momentum space. The SSFMs are calculated by partitioning a region of transverse momentum space into a lattice of $M \times M$ equal-size bins, and counting the number of proton pairs per bin

$$F_2(M) = \left\langle \frac{1}{M^2} \sum_{i=1}^{M^2} n_i(n_i - 1) \right\rangle \bigg/ \left\langle \frac{1}{M^2} \sum_{i=1}^{M^2} n_i \right\rangle^2 , \qquad (1)$$

where n_i is the number of particles in the ith bin and M^2 is the total number of bins, and we average over bins and events ($\langle \dots \rangle$). In the case of a pure system exhibiting critical fluctuations, $F_2(M)$ is expected to scale with M, for large values of M, as a power-law

$$F_2(M) \sim M^{2\phi_2} , \qquad \phi_2 = \phi_{2,\text{cr}}^{\text{B}} = {}^5\!/_6 , \qquad (2)$$

where ϕ_2 is the intermittency index, and provided the freeze-out occurs at exactly the critical point [10].

Noisy experimental data require the subtraction of a background of uncorrelated and misidentified protons, which is achieved through the construction of correlation-free mixed events. A correlator $\Delta F_2(M)$ can then

be defined in terms of the moments of data and mixed events. We define $\lambda(M) \equiv \langle n_{\mathrm{b}} \rangle / \langle n \rangle$ as the ratio of background to data average per bin particle multiplicities. In the limiting case of a dominant background, $\lambda(M) \lesssim 1$, the critical behaviour is expected to be revealed in the approximate correlator estimate (e),

$$\Delta F_2^{\mathrm{e}}(M) \simeq F_2^{\mathrm{d}}(M) - F_2^{\mathrm{m}}(M) \,, \tag{3}$$

where mixed event (m) moments are simply subtracted from data (d) moments [9]. $\Delta F_2(M)$ should then scale as a power law, $\Delta F_2(M) \sim M^{2\phi_2}$, in a limited range, with the same intermittency index as the pure critical system.

Furthermore, calculation of SSFMs is smoothed by averaging over many lattice positions (lattice averaged SSFMs, see Ref. [9]). An improved estimation of statistical errors of SSFMs is achieved by the use of the bootstrap method [11–13], whereby the original set of events is resampled with replacement [9].

It is to be noted that, while individual $F_2(M)$ errors and confidence intervals can be estimated fairly well through the bootstrap, $F_2(M)$ errors for different M are correlated, since the same data set is used in the calculation of all $F_2(M)$. Additional information about error correlations is contained in the full $F_2(M)$ correlation matrix, which can also be estimated through the bootstrap (see, for example, Ref. [11]). Furthermore, ϕ_2 and its accompanying uncertainties should properly be determined not through a simple χ^2-fit, but through a correlated fit. Unfortunately, such fits are plagued by instabilities [14]. We, therefore, resort to other methods in order to estimate ϕ_2 uncertainties, such as individually fitting bootstrap samples to obtain a distribution of ϕ_2 values and corresponding confidence intervals; however, present quoted ϕ_2 uncertainties should be considered tentative.

A proton generating modification of the Critical Monte Carlo (CMC) code [5, 10] is used to simulate a system of critically correlated protons, which are mixed with a non-critical background to study the effects on the quality of intermittency analysis.

3. Results

3.1. NA49 data analysis results

Proton intermittency analysis was first performed on data collected by the NA49 experiment [9]. Three collisions systems of different size were analysed: "C"+C, "Si"+Si and Pb+Pb at mid-rapidity, at the maximum SPS energy of $158A$ GeV/c. Figure 1 shows SSFMs $F_2(M)$ and $\Delta F_2(M)$ for the analysed NA49 systems. No intermittency was detected in "C"+C and Pb+Pb; by contrast, the "Si"+Si system exhibits power-law fluctuations

compatible with criticality. For the latter, the intermittency index value was estimated, through the bootstrap, as $\phi_{2,\text{B}} = 0.96^{+0.38}_{-0.25}(\text{stat.})\pm0.16(\text{syst.})$ [9].
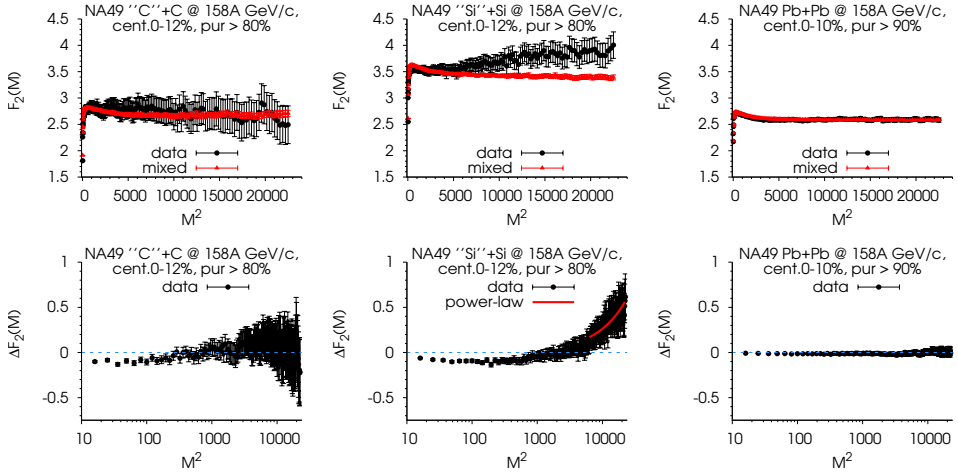

Fig. 1. Top row: $F_2(M)$ of original (filled circles) and mixed events (filled triangles) for NA49 "C"+C (left), "Si"+Si (middle) and Pb+Pb (right) collisions at $158A$ GeV/c ($\sqrt{s_{NN}} = 17.3$ GeV). Bottom row: $\Delta F_2^{\text{e}}(M)$ for the corresponding systems. The "Si"+Si system (middle) is fitted with a power-law, $\Delta F_2^{\text{e}}(M\,;\,\mathcal{C},\phi_2) = \text{e}^{\mathcal{C}}\left(M^2\right)^{\phi_2}$, for $M^2 > 6000$.

Furthermore, the behaviour of SSFMs in NA49 "Si"+Si was simulated through the "noisy CMC" code. Critical protons produced by the aforementioned CMC code can be mixed with random (uncorrelated) protons; the ratio λ of background-to-total protons is a free parameter of the simulation, and can be adjusted so that simulated SSFMs approximate experimental ones. Figure 2 (a) shows the moments $F_2(M)$ of NA49 "Si"+Si data compared to a $\lambda = 99\%$ noise-contaminated CMC set, which match the former with fair accuracy. In Fig. 2 (b), $\Delta F_2^{\text{e}}(M)$ is shown for the same CMC set, as well as the pure CMC; we notice that $\Delta F_2^{\text{e}}(M)$ of noisy CMC reproduces the slope (intermittency index ϕ_2) of the pure CMC critical set, although their moments differ by orders of magnitude. Finally, Fig. 2 (c) shows the distribution of ϕ_2 values across different bootstrap samples for the same noisy CMC set. The large uncertainty of ϕ_2 values in the NA49 "Si"+Si system is reproduced in noisy CMC, and can now be understood as a result of mixing with background protons; the median ϕ_2 value approximates the theoretically expected intermittency index of the pure CMC. CMC simulations justify our assumption that we are well within the dominant background region in the NA49 data sets, and thus the $\Delta F_2^{\text{e}}(M)$ approximation to the correlator is valid.
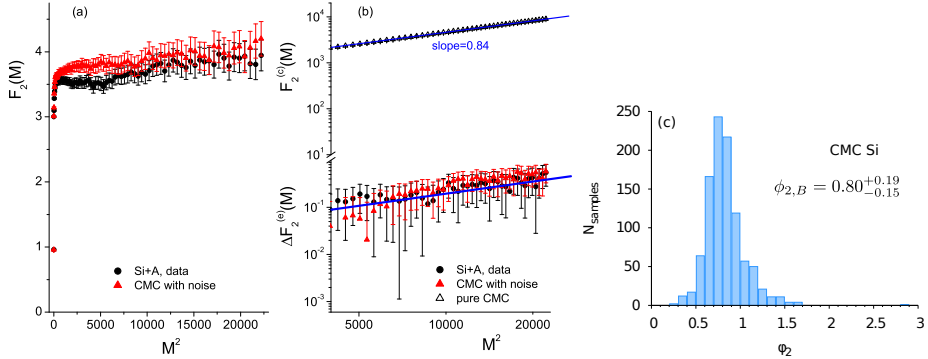
Fig. 2. (a) $F_2(M)$ of NA49 "Si"+Si data (filled cirles) and noisy CMC simulated collisions (filled triangles) with $\lambda = 99\%$ background noise. (b) $F_2^c(M)$ for pure CMC system (open triangles), as well as the correlator $\Delta F_2^e(M)$ for noisy CMC. $\Delta F_2^e(M)$ is also shown for NA49 "Si"+Si data for comparison. The solid lines correspond to the theoretically expected slope $\phi_{2,\mathrm{cr}}^{\mathrm{B}}$. (c) $\phi_{2,\mathrm{B}}$ bootstrap distribution for noisy "Si"+Si CMC. Asymmetric errors correspond to a 67% confidence interval.

3.2. NA61/SHINE Be+Be preliminary data analysis

Guided by the positive NA49 "Si"+Si result, we look for intermittency in collisions of medium-sized nuclei recorded within the successor experiment NA61/SHINE. Our two main candidate NA61 systems for study are $^7\mathrm{Be} + ^9\mathrm{Be}$ and $^{40}\mathrm{Ar} + ^{45}\mathrm{Sc}$ at $150A$ GeV/c. Preliminary analysis of NA61/SHINE Be+Be at $150A$ GeV/c was presented in [15]. We analysed a set of about 160K, 12% most central events, with an average proton multiplicity of 1.48 ± 0.74 in the mid-rapidity range, excluding events with a zero proton multiplicity in this range. In Fig. 3, intermittency analysis results are shown for NA61/SHINE Be+Be data. $F_2(M)$ for data and mixed events overlap; thus, $\Delta F_2(M)$ fluctuates around zero, and no intermittency effect is observed.
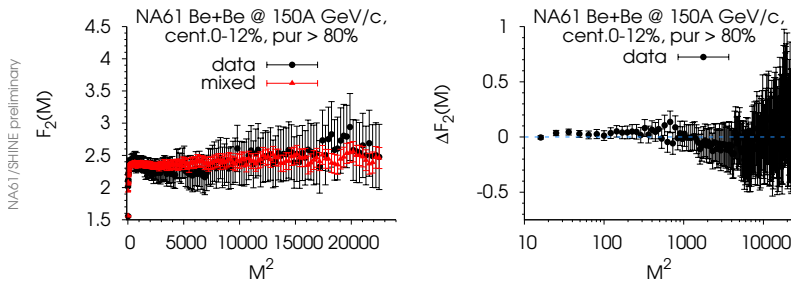

Fig. 3. Left: $F_2(M)$ of protons in NA61/SHINE Be+Be collisions at $\sqrt{s_{NN}} = 16.8$ GeV, for data (black circles) and mixed events (red triangles). Right: $\Delta F_2^e(M)$ for the corresponding system.

Based on noisy Critical Monte Carlo simulation of the Be+Be system, we estimate an upper limit of the order of 0.3% for the fraction of critical protons in Be+Be data to be consistent with the experimental observation.

3.3. NA61/SHINE Ar+Sc intermittency analysis at 150A GeV/c

We now turn to the main focus of our present work, the intermittency analysis performed on the NA61/SHINE ^{40}Ar + ^{45}Sc system, first presented in [16]. Following our intuition that different collision centralities may correspond to distinct freeze-out conditions, we partitioned the available data into three subsets corresponding to 0–5%, 5–10% and 10–15% most central collisions, determined by projectile spectator energy. We found, additionally, that proton purity selection affects the profile of SSFMs considerably; we thus performed a full scan in proton purity, at thresholds of 80%, 85%, and 90%.

Table I summarizes the Ar+Sc statistics for all centralities and for 90% proton purity threshold. The average total proton multiplicities are in all cases above the minimum required threshold of 2; however, event statistics is rather low, of the order of 150K events. Consequently, SSFMs statistical uncertainties are rather large.

TABLE I

Event statistics and average proton multiplicity in the analysis window for the 3 analysed centralities in NA61/SHINE Ar+Sc at 150A GeV/c. The 3$^{\rm rd}$ column gives proton multiplicities after dropping empty (zero multiplicity) events; the 4$^{\rm th}$ column, including zero multiplicity events.

Centrality	#events	$\langle p \rangle_{|p_{\rm T}| \leq 1.5 \ {\rm GeV}, \, |y_{\rm CM}| \leq 0.75}$	
		Non-empty	With empty
0–5%	144,362	3.44 ± 1.79	3.30 ± 1.89
5–10%	148,199	3.00 ± 1.61	2.79 ± 1.73
10–15%	142,900	2.81 ± 1.53	2.58 ± 1.66

In order to proceed with an intermittency analysis properly, a final potential risk must be addressed: the candidate proton selection must be as free as possible of split tracks, which are parts of the same track erroneously reconstructed as two separate tracks which are close in the detector, as well as in momentum space. Such tracks can greatly mislead an analysis focused on pair correlation; we remove them through single track quality cuts, by imposing a minimum separation distance of accepted tracks in the detector, and, finally, through a cut in the $q_{\rm inv}$ value of proton pairs

$$q_{\rm inv}(p_i, p_j) \equiv \tfrac{1}{2}\sqrt{-(p_i - p_j)^2} \,, \tag{4}$$

where p_i is the 4-momentum of the ith track. We calculate the q_{inv} distributions for original data, as well as for mixed events pairs, and then form the ratio $P(q_{\text{inv}})^{\text{d}}/P(q_{\text{inv}})^{\text{m}}$ of their p.d.f.s. Figure 4 shows the q_{inv} ratios in Ar+Sc per centrality bin. The canonical form of the q_{inv} ratio is predicted [17] to have a peak around 20–30 MeV/c due to strong interactions and to be suppressed for lower q_{inv} due to the Fermi–Dirac effects and Coulomb repulsion; an enhancement of the ratio at very low q_{inv} would then signify possible split track contamination that must be removed. Based on the observed q_{inv} ratios for Ar+Sc, we impose a universal cutoff of $q_{\text{inv}} > 7$ MeV/c to all sets before analysis.
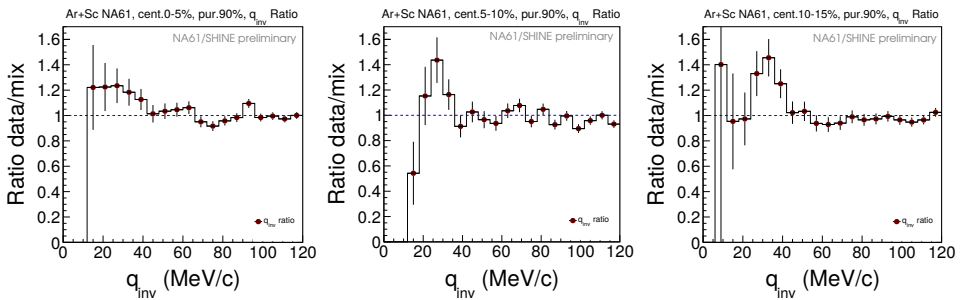

Fig. 4. The ratio $P(q_{\text{inv}})^{\text{d}}/P(q_{\text{inv}})^{\text{m}}$ for a 90% minimum proton purity selection, for NA61 Ar+Sc collisions at $150A$ GeV/c, at 0–5% (left), 5–10% (middle) and 10–15% (right) centrality range.

A preliminary analysis is then performed on the final selection of protons (after the application of all pair cuts). For all proton pairs, in the original set of events as well as in mixed events, the transverse momentum distance Δp_{T} is calculated, in direct correspondence to q_{inv}

$$\Delta p_{\text{T}} \equiv \tfrac{1}{2}\sqrt{(p_{X_1} - p_{X_2})^2 + (p_{Y_1} - p_{Y_2})^2}\,. \tag{5}$$

Figure 5 shows the distribution ratios $P(\Delta p_{\text{T}})^{\text{d}}/P(\Delta p_{\text{T}})^{\text{m}}$ for the 3 centralities in Ar+Sc, compared to the corresponding ratios for a simulation of the Ar+Sc system via the EPOS event generator [18]. We see evidence of power-law scaling for $\Delta p_{\text{T}} \to 0$ for middle-central (5–10% and 10–15%) NA61/SHINE Ar+Sc collisions; no clear power-law structure is visible in the corresponding EPOS spectra.

Finally, we calculate the SSFMs for each NA61/SHINE data subset in the 3×3 centrality and proton purity selections. Figure 6 shows the results per centrality bin, for the case of 90% proton purity. As indicated by the preliminary Δp_{T} probe, we observe that the $F_2(M)$ of data rise significantly above those of mixed events for the 10–15% centrality case; the effect is weaker but
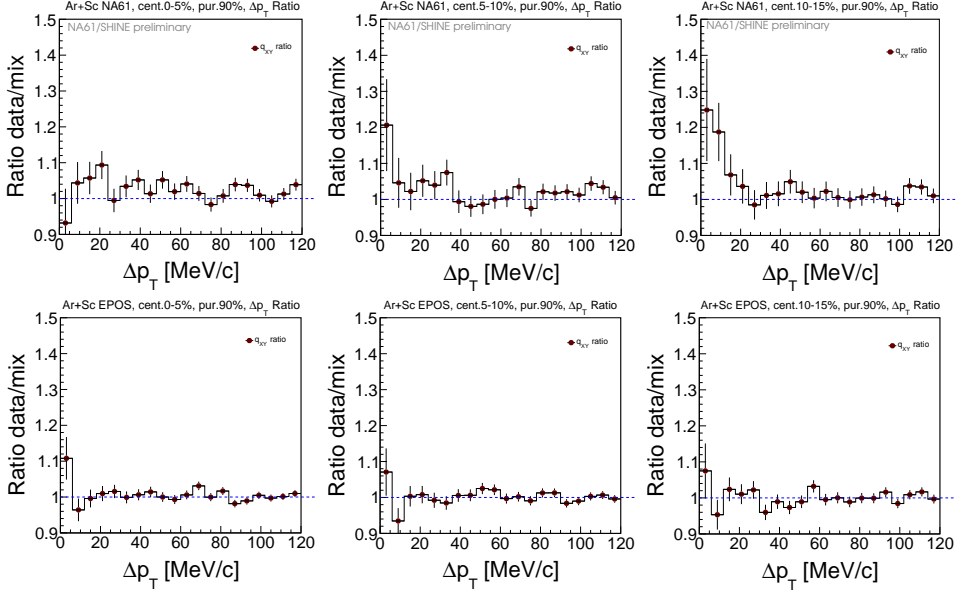
Fig. 5. Top row: The ratio $P(\Delta p_T)^d/P(\Delta p_T)^m$ for a 90% minimum proton purity selection, for NA61 Ar+Sc collisions at $150A$ GeV/c, at 0–5% (left), 5–10% (middle) and 10–15% (right) centrality range. Bottom row: Corresponding Δp_T ratios for EPOS [18] simulated Ar+Sc collisions of the same centrality.

still present in 5–10% most central collisions, while central (0–5%) collisions show a total overlap of moments (no intermittency effect). However, the magnitude and M-bin correlation of $\Delta F_2(M)$ uncertainties prevent us from properly estimating the quality of the power-law, or calculating confidence intervals for ϕ_2, for the time being.

Figure 7 shows $F_2(M)$ and $\Delta F_2(M)$ calculated for EPOS simulations of the corresponding systems. We observe significant overlap of moments for data and mixed events; EPOS fails to reproduce the effect seen in NA61/SHINE $\Delta F_2(M)$ for middle-central collisions. It must be noted that the power-law curves (solid red lines) are drawn solely to guide the eye; fitting a power-law is meaningless due to the prevalence of negative $\Delta F_2(M)$ values.

Figures 8 and 9 summarize the scan in centrality and proton purity for NA61/SHINE Ar+Sc data. In general, we see a tendency for increased $\Delta F_2(M)$ scaling as we increase peripherality and proton purity.
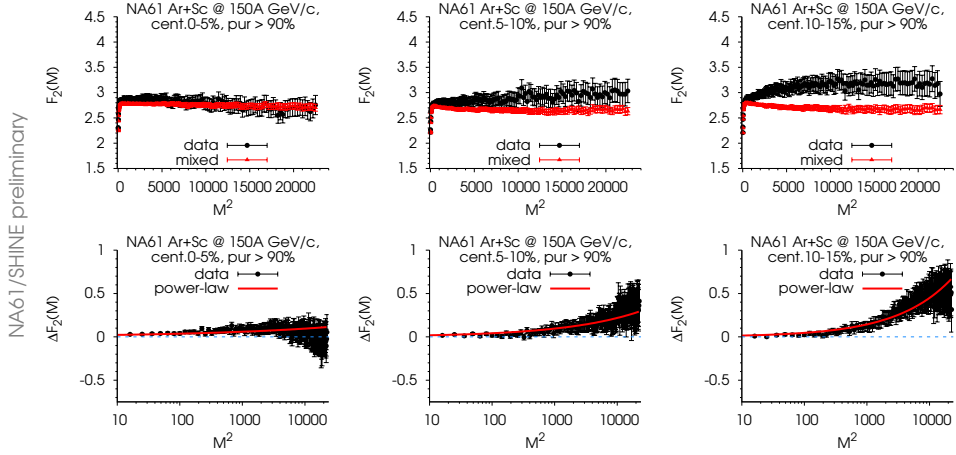
Fig. 6. Top row: $F_2(M)$ of original (filled circles) and mixed events (filled triangles) for NA61 Ar+Sc collisions at 0–5% (left), 5–10% (middle) and 10–15% (right) centrality at $150A$ GeV/c ($\sqrt{s_{NN}} = 16.8$ GeV). Bottom row: $\Delta F_2^{\mathrm{e}}(M)$ for the corresponding systems. The solid curves are drawn to guide the eye and correspond to power-law scaling functions, $\Delta F_2^{\mathrm{e}}(M\;;\;\mathcal{C},\phi_2) = \mathrm{e}^{\mathcal{C}} \times (M^2)^{\phi_2}$, with parameters: (left) $\phi_2 = 0.21$, $\mathcal{C} = -4.27$; (middle) $\phi_2 = 0.36$, $\mathcal{C} = -4.84$; (right) $\phi_2 = 0.49$, $\mathcal{C} = -5.4$.
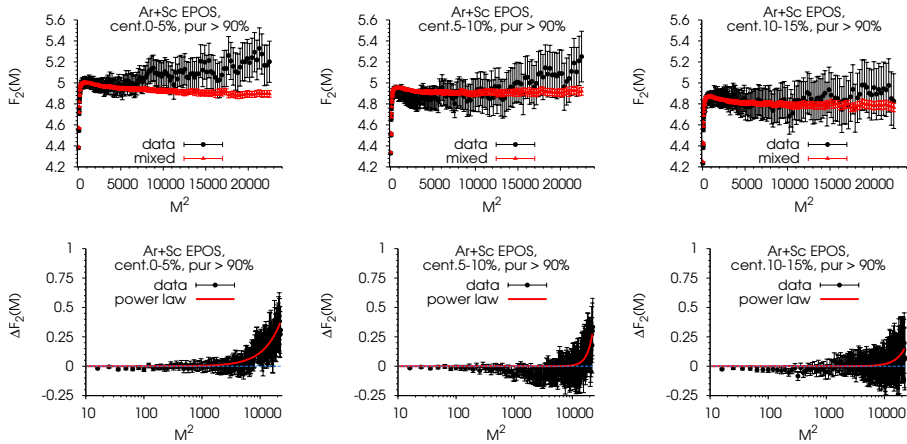

Fig. 7. Top row: $F_2(M)$ of original (filled circles) and mixed events (filled triangles) for EPOS Ar+Sc collisions at 0–5% (left), 5–10% (middle) and 10–15% (right) centrality at $150A$ GeV/c ($\sqrt{s_{NN}} = 16.8$ GeV). Bottom row: $\Delta F_2^{\mathrm{e}}(M)$ for the corresponding systems. The solid curves are drawn to guide the eye and correspond to power-law scaling functions, $\Delta F_2^{\mathrm{e}}(M\;;\;\mathcal{C},\phi_2) = \mathrm{e}^{\mathcal{C}} \left(M^2\right)^{\phi_2}$.
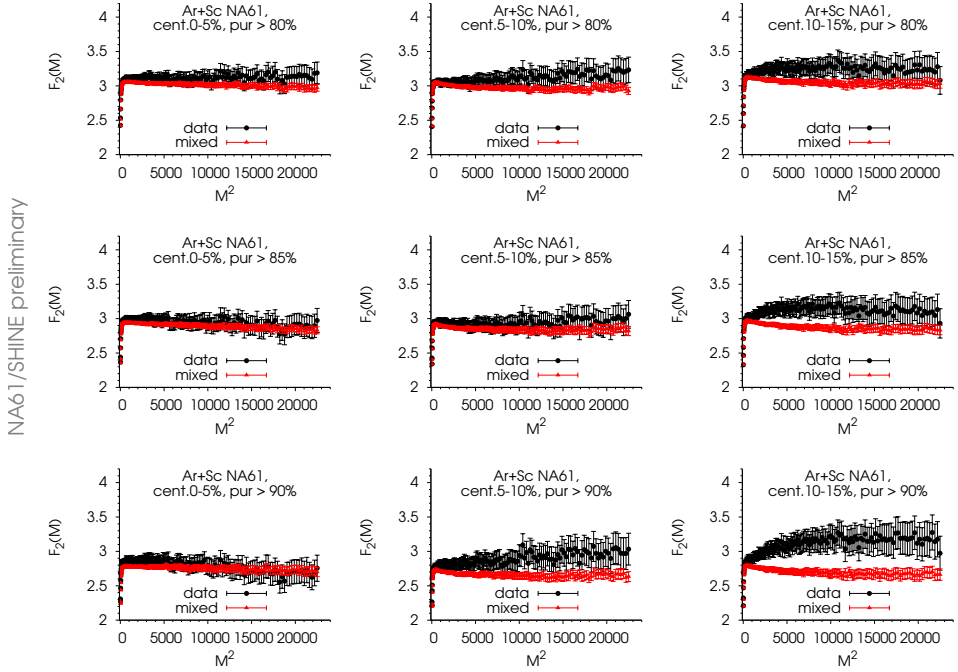
Fig. 8. $F_2(M)$ of original (filled circles) and mixed events (filled triangles) for NA61 Ar+Sc collisions at 0–5% (left), 5–10% (middle) and 10–15% (right) centrality at $150A$ GeV/c, for 80% (top), 85% (center), and 90% (bottom) proton purity thresholds.

4. Summary and conclusions

Intermittency analysis in transverse momentum space is a powerful tool for detecting self-similar (power-law) fluctuations of the proton density, thus providing us with a promising set of observables for the detection of the critical point of strongly interacting matter. The intermittency analysis performed on NA49 "Si"+Si data at the maximum SPS energy already suggests the presence of a critical proton component of the order of 1%, with an estimated intermittency index value of $\phi_{2,\mathrm{B}} = 0.96^{+0.38}_{-0.25}$, overlapping with the critical QCD prediction, whereas no intermittency is observed in either the smaller "C"+C or the larger Pb+Pb system at the same collision energy. The preliminary analysis of the NA61/SHINE central Be+Be system at $150A$ GeV/c consistently shows no positive result.

We see the first indication of a non-trivial intermittency effect in NA61/SHINE in our preliminary analysis of Ar+Sc collisions at $150A$ GeV/c. We see evidence of power-law scaling in the SSFMs $\Delta F_2(M)$ of Ar+Sc collisions; the quality of the effect seems to increase for less cen-
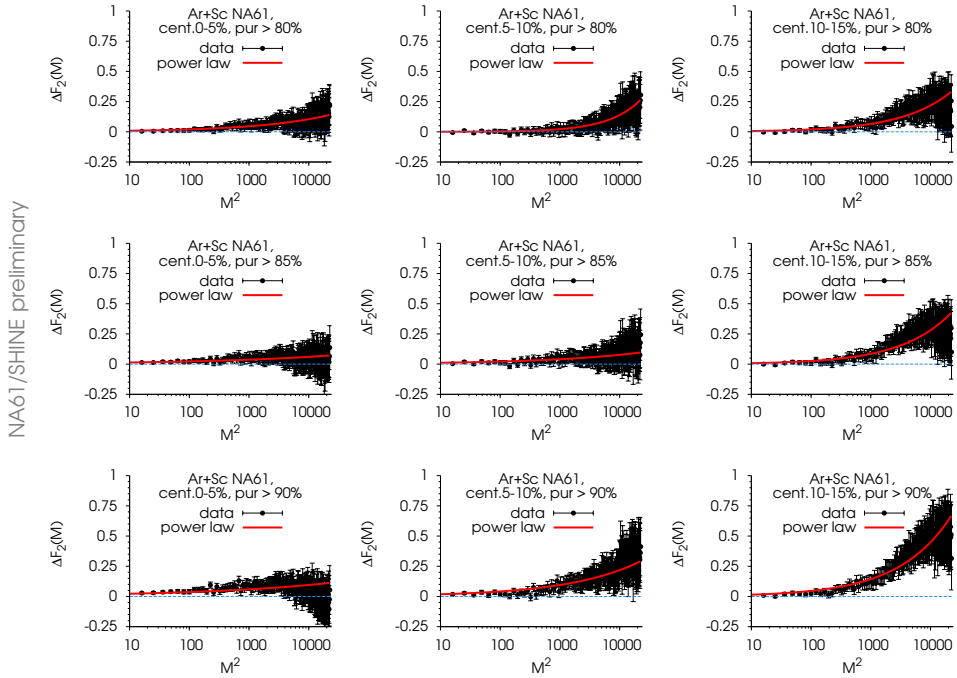
Fig. 9. $\Delta F_2(M)$ of original (filled circles) and mixed events (filled triangles) for NA61 Ar+Sc collisions at 0–5% (left), 5–10% (middle) and 10–15% (right) centrality at $150A$ GeV/c, for 80% (top), 85% (center), and 90% (bottom) proton purity thresholds.

tral collisions, as well as for increased proton purity thresholds, up to 90% purity. EPOS simulations of the corresponding systems fail to reproduce the effect. However, due to the magnitude of SSFMs uncertainties, and the fact that $F_2(M)$ values for distinct M are correlated, the quality of $\Delta F_2(M)$ power-law scaling remains still to be established, and an estimation of ϕ_2 confidence intervals is still pending.

A continued, final analysis of the total available statistics of NA61/SHINE Ar+Sc data, and its extension to other system sizes (Xe+La) and energies of the NA61/SHINE program will hopefully lead to an accurate determination of the critical point location.

REFERENCES

[1] K. Fukushima, T. Hatsuda, *Rep. Prog. Phys.* **74**, 014001 (2011).

[2] C. Alt *et al.*, *Phys. Rev. C* **75**, 064904 (2007); **78**, 034914 (2008).

[3] L. Adamczyk *et al.*, *Phys. Rev. Lett.* **112**, 032302 (2014).

[4] T. Anticic *et al.*, *Phys. Rev. C* **70**, 034902 (2004); **79**, 044904 (2009).

[5] N.G. Antoniou *et al.*, *Nucl. Phys. A* **693**, 799 (2001).

[6] N.G. Antoniou, Y.F. Contoyiannis, F.K. Diakonos, G. Mavromanolakis, *Nucl. Phys. A* **761**, 149 (2005).

[7] Y. Hatta, M.A. Stephanov, *Phys. Rev. Lett.* **91**, 102003 (2003).

[8] T. Vicsek, *Fractal Growth Phenomena*, World Scientific, Singapore 1989, ISBN 9971-50-830-3.

[9] T. Anticic *et al.*, *Eur. Phys. J. C* **75**, 587 (2015).

[10] N.G. Antoniou, F.K. Diakonos, A.S. Kapoyannis, K.S. Kousouris, *Phys. Rev. Lett.* **97**, 032002 (2006).

[11] W.J. Metzger, Estimating the Uncertainties of Factorial Moments, HEN-455, 2004.

[12] B. Efron, *Ann. Stat.* **7**, 1 (1979).

[13] T. Hesterberg *et al.*, *Bootstrap Method and Permutation Tests*, W.H. Freeman & Co., USA, 2003, ISBN-10:0716757265.

[14] C. Michael, *Phys. Rev. D* **49**, 2616 (1994).

[15] N. Davis, N. Antoniou, F.K. Diakonos, *PoS* **CPOD2017**, 054 (2018).

[16] N. Davis [NA61/SHINE Collaboration], Recent Results from Proton Intermittency Analysis in Nucleus–Nucleus Collisions from NA61 at CERN SPS, The Critical Point and Onset of Deconfinement Conference "CPOD2018", Corfu, Greece, September 24–28, 2018.

[17] S.E. Koonin, *Phys. Lett. B* **70**, 43 (1977).

[18] K. Werner, F. Liu, T. Pierog, *Phys. Rev. C* **74**, 044902 (2006).